

Multimodal Prototype-Enhanced Network for Few-Shot Action Recognition

Xinzhe Ni, Hao Wen, Yong Liu, Yatai Ji, Yujiu Yang
 Shenzhen International Graduate School, Tsinghua University
 {nxz22, wenh22, liu-yong20, jyt21}@mails.tsinghua.edu.cn
 yang.yujiu@sz.tsinghua.edu.cn

Abstract

Current methods for few-shot action recognition mainly fall into the metric learning framework following ProtoNet. However, they either ignore the effect of representative prototypes or fail to enhance the prototypes with multimodal information adequately. In this work, we propose a novel **Multimodal PRototype-ENhanced Network (MORN)** to use the semantic information of label texts as multimodal information to enhance prototypes, including two modality flows. A CLIP visual encoder is introduced in the visual flow, and visual prototypes are computed by the Temporal-Relational CrossTransformer (TRX) module. A frozen CLIP text encoder is introduced in the text flow, and a semantic-enhanced module is used to enhance text features. After inflating, text prototypes are obtained. The final multimodal prototypes are then computed by a multimodal prototype-enhanced module. Besides, there exist no evaluation metrics to evaluate the quality of prototypes. To the best of our knowledge, we are the first to propose a prototype evaluation metric called **PRototype SIMilarity DIfference (PRIDE)**, which is used to evaluate the performance of prototypes in discriminating different categories. We conduct extensive experiments on four popular datasets. MORN achieves state-of-the-art results on HMDB51, UCF101, Kinetics and SSv2. MORN also performs well on PRIDE, and we explore the correlation between PRIDE and accuracy.

1. Introduction

Few-shot learning is a challenging problem in computer vision because of the scarcity of labeled samples. Among few-shot learning problems, few-shot action recognition is one of the hardest problems for the complicated temporal evolution of videos. Most of the methods [3, 4, 11, 19, 23, 26, 33, 43, 50, 51, 56, 57, 59, 61, 62] for few-shot action recognition mainly fall into the metric-learning framework including a meta-training stage and a meta-test stage. Among various metric-learning works, ProtoNet [39] has been followed by many works and has far-reaching influence. It

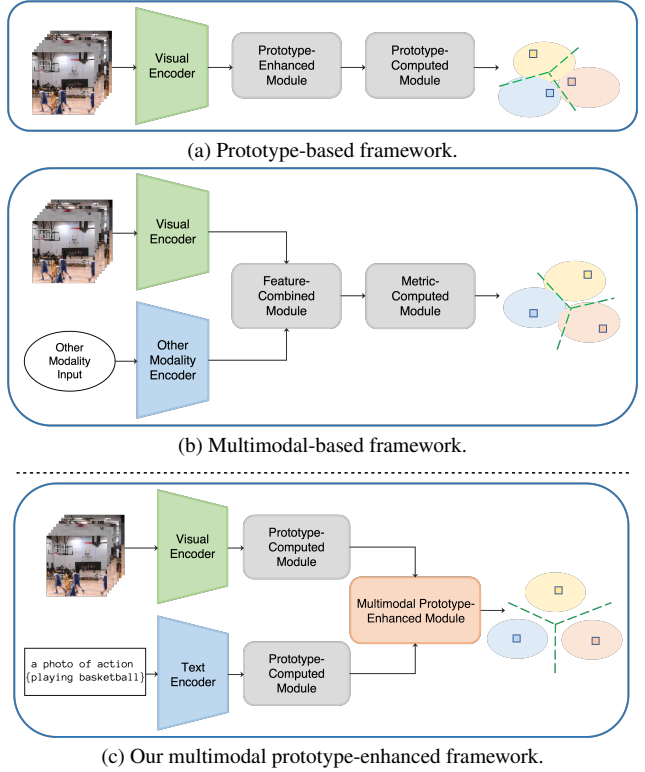


Figure 1. Existing metric-learning framework (a) and (b) and our multimodal prototype-enhanced framework (c) for few-shot action recognition. The oval indicates the distribution of samples and the rectangle inside indicates the prototype in the final matching space. (a) enhances the prototype but ignores the multimodal information. (b) uses multimodal information but combines two modalities on the feature level. Our multimodal prototype-enhanced framework (c) pays attention to both the semantic information of label texts and the prototype enhancement.

proposes the prototype as a representation of each category in a few-shot learning scenario, and the key objective is to obtain representative prototypes. It is efficient for distance computing and accurate for classification with prototypes. There exist two metric-learning frameworks for few-shot

action recognition. One is the prototype-based framework as shown in Fig. 1a, which uses a certain enhanced strategy to compute more representative prototypes. However, methods with the prototype-based framework [23, 33, 62] only use the visual modality of videos and thus cannot take full advantage of the scarce video samples. The other is the multimodal-based framework as shown in Fig. 1b. It combines the information of two modalities to obtain a better distance metric. However, methods with the multimodal-based framework [11, 57] ignore the importance of prototypes and only combine the two modalities on the feature level. As a result, none of them are comprehensive and fail to obtain representative prototypes.

In this case, we propose a multimodal prototype-enhanced framework to enhance prototypes with the multimodal information as shown in Fig. 1c. Inspired by ActionCLIP [49], there is abundant semantic information in label texts to assist the classification. For example, if one is given several short videos of “lifting up one end of something” without being told what action it is, he may not find the same pattern in a short time. Instead, it is much easier to distinguish them from other actions when knowing the exact label. Based on this fact, we use the semantic information of label texts to enhance prototypes and assist the classification. Besides, there exist no prototype evaluation metrics to evaluate the quality of prototypes. It is necessary to propose a prototype evaluation metric and further evaluate the multimodal prototypes.

To this end, we propose a novel **Multimodal PRototype-Enhanced Network (MORN)** based on our proposed framework. It is simple but well-performed, including two modality flows. In the visual flow, we introduce a CLIP [34] visual encoder to obtain more reliable features of video samples. CLIP has superior zero-shot learning ability and has been extended to few-shot classification by several works [12, 58, 60]. Then, visual prototypes are computed by TRX [33] baseline model. In the text flow, we first make discrete templates like “a photo of action { }” as text prompts. Some works [34, 49] indicate that text prompts can help bridge the distribution gap with the CLIP pre-trained model and enrich the semantic information of only one or several label words. Then, we introduce a frozen CLIP text encoder and use the prompted label texts as inputs. After that, we introduce a semantic-enhanced (SE) module to obtain text features with more reliable semantic information and the outputs are regarded as text prototypes. Finally, we combine visual prototypes and text prototypes to obtain more representative prototypes in a multimodal prototype-enhanced (MPE) module. The final multimodal prototypes are used during the distance computation with query videos.

To further evaluate the effectiveness of prototypes, we propose a metric to evaluate the quality of prototypes called **PRototype Similarity Difference (PRIDE)**. To the best of

our knowledge, PRIDE is the first metric to evaluate the quality of prototypes on the ability of discriminating different categories. Inspired by [55], we first compute the real prototype of each category of all samples in the meta-test stage. Then, the similarities of the multimodal prototype in each episode with all real prototypes are computed. The difference between its own category and the average of other categories is used to evaluate the effectiveness of the prototype. More details will be further illustrated in Sec. 3.4.

Our contributions can be summarized as follows:

- We use the semantic information of label texts to enhance the prototypes and propose a simple but well-performed Multimodal Prototype-Enhanced Network (MORN).
- Rather than obtaining more reliable features, we focus on computing more representative prototypes with multimodal information. Moreover, we are the first to propose a prototype evaluation metric called Prototype Similarity Difference (PRIDE) to the best of our knowledge.
- We conduct extensive experiments on four popular action recognition datasets. MORN achieves state-of-the-art results on HMDB51, UCF101, Kinetics and SSv2.

2. Related Work

2.1. Few-Shot Image Classification

Few-shot image classification methods can be widely divided into three categories: augmentation-based, optimization-based and metric-based.

Augmentation-based methods. The objective of these methods is to use augmentation techniques or extra data to increase samples for training and improve the diversity of data. Some prior attempts are intuitive, including [32, 37]. Besides direct data augmentation, some works focus on the semantic feature level, including [6, 7]. Rather than applying augmentation techniques, [30, 31] introduce a GAN [14] architecture to generate extra images based on the text description to compensate for the lack of data.

Optimization-based methods. The objective of these methods is to train a model under the meta-learning framework so that it can adapt to novel tasks with only a few optimization steps. [1, 16, 24, 27, 38] utilize the meta-learner as an optimizer. MAML [10] and its variants [2, 20, 41] aim to learn a robust model initialization.

Metric-based methods. The objective of these methods is to learn feature embeddings under a certain distance metric with a better generalization ability. Samples of novel categories can be accurately classified via a nearest neighbor classifier with different distance metrics such as co-

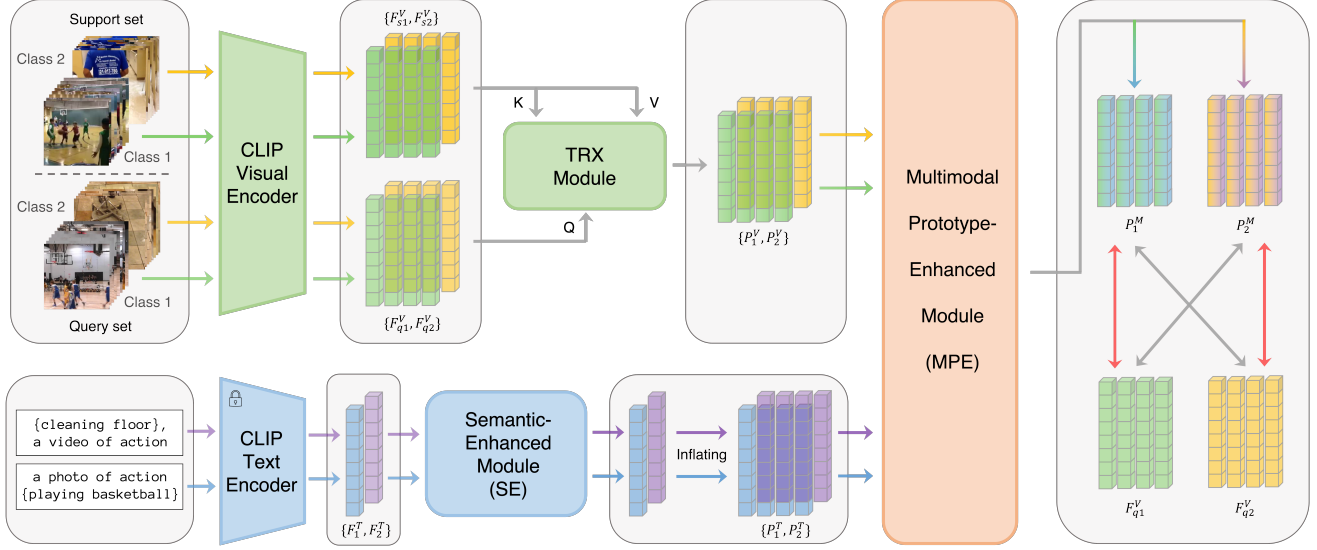


Figure 2. Overview of our proposed MORN on a 2-way 1-shot problem with 1 video for each category in the query set. In the visual flow, a CLIP visual encoder is first introduced on videos in both the support set and the query set with L frames to obtain video features. Then, support video features regarded as key and value and query video features regarded as query are passed to the Temporal-Relational CrossTransformer (TRX) module to compute visual prototypes. In the text flow, a frozen CLIP text encoder is first introduced on the prompted label texts. Then, the semantic features of label texts are passed to a semantic-enhanced (SE) module and are inflated to compute text prototypes. The visual prototypes and the text prototypes are combined through a multimodal prototype-enhanced (MPE) module. The final multimodal prototypes are obtained and are used during the distance computation with query videos.

sine similarity [47, 53], Euclidean distance [39, 54], non-linear metric with CNNs [18, 25, 42] or graph neural networks [13, 21, 52]. Our work falls into the metric-learning framework and aims to solve a more complicated few-shot video action recognition problem.

2.2. Few-Shot Action Recognition

Most of the methods for few-shot action recognition mainly fall into the metric-learning framework. More specifically, we divide them into three categories: feature-based, multimodal-based and prototype-based.

Feature-based methods. The objective of these methods is to obtain reliable video features or apply an effective alignment strategy. CMN [61], TARN [3], OTAM [4] and ARN [56] make preliminary attempts to obtain reliable video features for classification. ITANet [59] introduces a video representation based on a self-attention mechanism and an implicit temporal alignment. MASTAF [26] uses self-attention and cross-attention mechanisms to obtain reliable spatial-temporal features. MT-FAN [51] designs a motion modulator and a segment attention mechanism, and conducts a temporal fragment alignment. STRM [43] proposes a local patch-level and a global frame-level enrichment module. Similarly, HyRSM [50] proposes a hybrid relation module to enrich video features.

Multimodal-based methods. The objective of these methods is to use multimodal information to assist classification

under the metric-learning framework. AMeFu-Net [11] introduces depth information as an other modality to assist classification. [57] also uses the semantic information of label texts as ours and is similar to our multimodal setting. However, it fails to apply a feature extractor with a good multimodal initialization and ignores the importance of prototypes.

Prototype-based methods. Prototype is the representation of each category and is proposed by ProtoNet [39] in a few-shot learning scenario. The objective of these methods is to compute representative prototypes by some prototype-enhanced strategies with unimodal information for classification. ProtoGAN [23] generates extra samples by using a conditional GAN with category prototypes. PAL [62] matches a prototype with all the query samples instead of matching a query sample with the space of prototypes. TRX [33] is our baseline model and is the most relevant to our work. It applies CrossTransformer [9] to a few-shot action recognition scenario and thus obtains query-specific category prototypes. The details of TRX will be further illustrated in Sec. 3.2.

In addition, CPMT [19] can be divided into both multimodal-based and prototype-based methods. It uses object features as multimodal information and compound prototypes. Our work also utilizes multimodal information and computes representative prototypes. Furthermore, we notice the remarkable effect of the semantic information of

label texts and the prototype-enhanced strategy. As a result, our proposed MORN achieves state-of-the-art results and will be shown in Sec. 4.1.

3. Method

3.1. Problem formulation

There are two sets in the N -way K -shot few-shot scenario: a support set $S_K^N = \{s_1^1, \dots, s_K^1, \dots, s_1^N, \dots, s_K^N\}$ and a query set $Q_M^N = \{q_1^1, \dots, q_M^1, \dots, q_1^N, \dots, q_M^N\}$, where N denotes the number of different action categories, K denotes the number of videos each category in the support set and M denotes the number of videos each category in the query set. The objective of few-shot action recognition is to learn a model with great generalization ability using only a few video samples. Specifically, the model classifies a completely novel query action to the right category by matching it with the most similar video in the support set. Meanwhile, the whole dataset is divided into a base dataset $C_{base} = \{(x_i, y_i)\}_{i=1}^{|C_{base}|}$ and a novel dataset $C_{novel} = \{(x_i, y_i)\}_{i=1}^{|C_{novel}|}$, where y_i is the action category of a video sample x_i . Note that the categories of C_{base} and C_{novel} are sample-wise non-overlapping, i.e. $C_{base} \cap C_{novel} = \emptyset$. To make full use of the few video samples, we follow the episode training manner [47]. Each episode contains K videos in the support set and M videos in the query set of N categories.

3.2. TRX baseline

Our work adopts Temporal-Relational CrossTransformer (TRX) [33] as baseline. It applies CrossTransformer [9] to the few-shot action recognition scenario and obtains query-specific category prototypes. CrossTransformer combines the information of support images and query images to find their spatial correspondence through an attention operation. TRX further samples ordered sub-sequences of video frames called tuples and thus can capture higher-order temporal relationships.

To fully exploit the temporal relationships of a video with L frames, TRX firstly samples tuples of video frames:

$$\Pi_\omega = \{(v_1, \dots, v_\omega) \in \mathbb{N}^\omega, 1 \leq v_i < v_{i+1} \leq L\}, \quad (1)$$

where ω is the length or cardinality of a tuple and v_i is the i -th frame sampled from a video. For example, if $L = 8$ and $\omega = 2$, the number of tuples is $C_8^2 = 28$. The set of cardinalities is denoted as Ω . Regarding query tuples Π_ω^Q as query and support tuples Π_ω^S as key and value, TRX obtains the query-specific category prototypes P^N by an attention operation:

$$P^N = \text{Attention}(\Pi_\omega^Q, \Pi_\omega^S, \Pi_\omega^S). \quad (2)$$

Then, the distance of videos in the support set S_K^N and the query set Q_M^N is computed:

$$T(Q_M^N, S_K^N) = \sum_{\omega \in \Omega} \frac{1}{|\Pi_\omega|} \sum_{v \in \Pi_\omega} \|q_v - p_v^N\|, \quad (3)$$

where q_v denotes the query video and p_v^N denotes the prototype in an episode. The distances T are passed as logits to a cross-entropy loss during training. More details are demonstrated in the original article [33].

3.3. MORN

The overall architecture of our proposed MORN is shown in Fig. 2, including a visual flow, a text flow and a multimodal prototype-enhanced (MPE) module.

Visual flow. For each input video, we uniformly sample L frames as in [48]. The video s_k^n in the support set and q_m^n in the query set can be further denoted as:

$$\begin{aligned} s_k^n &= \{s_{k1}^n, \dots, s_{kL}^n\}, \\ q_m^n &= \{q_{m1}^n, \dots, q_{mL}^n\}, \end{aligned} \quad (4)$$

where $s_k^n, q_m^n \in \mathbb{R}^{L \times H \times W \times 3}$. H denotes the height and W denotes the width of an image. Then, we apply a pre-trained CLIP visual encoder for a better multimodal initialization. The visual features of each video frame $s_{ki}^n \in \mathbb{R}^{H \times W \times 3}$ in the support set and $q_{mi}^n \in \mathbb{R}^{H \times W \times 3}$ in the query set are defined as:

$$\begin{aligned} F_{sk}^V &= \{f_v(s_{k1}^n), \dots, f_v(s_{kL}^n)\}, \\ F_{qm}^V &= \{f_v(q_{m1}^n), \dots, f_v(q_{mL}^n)\}, \end{aligned} \quad (5)$$

where $F_{sk}^V, F_{qm}^V \in \mathbb{R}^{L \times d}$. The visual features of videos in the support set and the query set are denoted as:

$$\begin{aligned} F_s^V &= \{F_{s1}^V, \dots, F_{s(NK)}^V\}, \\ F_q^V &= \{F_{q1}^V, \dots, F_{q(NM)}^V\}, \end{aligned} \quad (6)$$

where $F_s^V \in \mathbb{R}^{NK \times L \times d}$, $F_q^V \in \mathbb{R}^{NM \times L \times d}$. Then, we compute visual prototypes of each episode through TRX:

$$P^V = \text{TRX}(F_q^V, F_s^V, F_s^V), \quad (7)$$

where $P^V \in \mathbb{R}^{NM \times d_p}$.

Text flow. In the training stage for each sample $(x_i, y_i) \in C_{base}$, we firstly make n_{temp} discrete templates $P_{temp} = \{p_1^{temp}, \dots, p_{n_{temp}}^{temp}\}$ of y_i as text prompts. Then, we apply a CLIP text tokenizer to obtain the tokenized text sequences T_i :

$$\begin{aligned} T_i &= \text{Tokenizer}(p_j^{temp} || y_i), \\ j &= 1, \dots, n_{temp}, i = 1, \dots, N, \end{aligned} \quad (8)$$

where $||$ denotes a concatenation operation. In the practical meta-training stage and meta-test stage, the template is

randomly selected once per episode. Then, the features of prompted label texts are obtained by a frozen CLIP text encoder:

$$F_i^T = f_t(T_i), x_i \in S_K^N \cup Q_M^N, \quad (9)$$

where $F_i^T \in \mathbb{R}^{1 \times d}$. To obtain text features with more reliable semantic information, we further apply a semantic-enhanced (SE) module $g(\cdot)$:

$$P_i^T = g(F_i^T), \quad (10)$$

where $P_i^T \in \mathbb{R}^{1 \times d_p}$ and a multi-head attention mechanism with 4 heads is utilized as $g(\cdot)$. Since different frames of videos in the same category have the same label, we simply inflate P_i^T of the same category to keep the same dimension with visual prototypes. Then, we obtain text prototypes P^T :

$$P^T = \{\underbrace{P_1^T, \dots, P_1^T}_M, \dots, \underbrace{P_N^T, \dots, P_N^T}_M\}, \quad (11)$$

where $P^T \in \mathbb{R}^{NM \times d_p}$.

Multimodal prototype-enhanced module. To utilize the multimodal information to enhance prototypes, we propose a simple but well-performed multimodal prototype-enhanced (MPE) module. The choice of the MPE module is flexible containing weighted average, multi-head attention and so on. Here, we apply the weighted average to compute multimodal prototypes:

$$P^M = (1 - \lambda)P^V + \lambda P^T, \quad (12)$$

where $P^M \in \mathbb{R}^{NM \times d_p}$ and λ is the multimodal enhanced hyper-parameter. The multimodal prototypes are used as the final prototypes. Then, distances are computed between multimodal prototypes and videos in the query set.

3.4. PRIDE

Denote the number of categories in the meta-test stage as N_{novel} . We first compute the real prototype by averaging all prototypes of the same category i in the novel dataset, which is based on [55]:

$$P_i^{real} = \frac{1}{|C_{novel}^i|} \sum_{(x,y) \in C_{novel}^i} P_i(x), \quad (13)$$

where $P_i(x)$ is the query-specific category prototype of video x and C_{novel}^i is the i -th category in C_{novel} . The whole set of real prototypes is denoted as:

$$P^{real} = \{P_1^{real}, \dots, P_{N_{novel}}^{real}\}. \quad (14)$$

Then, the cosine similarity can be computed between a given $P_i(x)$ and P_j^{real} :

$$Sim_j = sim(P_i(x), P_j^{real}), j = 1, \dots, N_{novel}, \quad (15)$$

where $sim(\cdot, \cdot)$ is the cosine similarity operation. The similarity of other categories is denoted as:

$$Sim_{other} = \frac{1}{N_{novel} - 1} \sum_{1 \leq j \neq i \leq N_{novel}} Sim_j. \quad (16)$$

We can now denote PRIDE as:

$$PRIDE_i(x) = Sim_i - Sim_{other}, (x, y) \in C_{novel}^i. \quad (17)$$

PRIDE is further used to evaluate the performance of prototypes in discriminating different categories. A higher value means a better discriminating ability.

4. Experiments

Datasets. We evaluate our method on four popular datasets: HMDB51 [22], UCF101 [40], Kinetics [5] and Something-Something V2 (SSv2) [15]. HMDB51 contains 51 action categories, each containing at least 101 clips for a total of 6,766 video clips. For HMDB51, we adopt the same protocol as [56] with 31/10/10 categories for train/val/test, respectively. UCF101 contains 101 action categories, each containing at least 100 clips for a total of 13,320 video clips. For UCF101, we also adopt the same protocol as [56] with 70/10/21 categories for train/val/test, respectively. Kinetics contains 400 action categories with 400 or more clips for each category. For Kinetics, we adopt the same protocol as [61] with 64/12/24 categories for train/val/test, respectively. SSv2 contains 220,847 videos of fine-grained actions with only subtle differences between different categories, which is regarded as a more challenging action recognition task. For SSv2, we adopt the same protocol as [4] with 64/12/24 categories for train/val/test, respectively.

Implementation details. Previous works [4, 19, 33, 43, 50, 51, 62] utilize a ResNet-50 [17] pre-trained on ImageNet [8] as the backbone. For a fair comparison, we utilize a pre-trained CLIP ResNet-50 as the visual backbone and a frozen CLIP text encoder based on a modified Transformer [46] in [35]. Each video is re-scaled to height 256 and uniformly sampled $L = 8$ frames as in [48]. We follow the TRX augmentation: random horizontal flipping and 224x224 crops in the meta-training stage, and only a center crop in the meta-test stage. We set $n_{temp} = 16$, $d_p = d = 1024$, $\Omega = \{2, 3\}$ and multimodal enhanced hyper-parameter $\lambda = 0.5$. According to [36], we use AdamW [28] as our optimizer with a learning rate of 10^{-5} for HMDB51, UCF101, Kinetics and SSv2. We randomly sample 10000 training episodes for HMDB51, UCF101 and Kinetics, while 75000 training episodes for SSv2. We average gradients and back-propagate once every 16 iterations. In the meta-test stage, we employ the standard 5-way 5-shot evaluation on all four datasets. We randomly sample 10000 test episodes and report the average accuracy.

Method	HMDB51	UCF101	Kinetics	SSv2	Average
ARN [56]	60.6	83.1	82.4	-	75.4
OTAM [4]	68.0	88.9	85.8	52.3	73.8
PAL [62]	75.8	95.2	87.1	62.6	80.2
TRX [33]	75.6	96.1	85.9	64.6	80.6
STRM [43]	77.3	96.9	86.7	68.1	82.3
HyRSM [50]	76	94.7	86.1	69.0	81.5
MT-FAN [51]	74.6	95.1	87.4	60.4	79.4
CPMT [19]	85.1	92.3	87.9	73.5	84.7
Ours: MORN (Weighted average)	<u>86.3</u>	<u>96.9</u>	<u>91.6</u>	71.1	<u>86.5</u>
Ours: MORN (Multi-head Attention)	87.1	97.7	94.6	<u>71.7</u>	87.8

Table 1. State-of-the-art comparison on four few-shot action recognition datasets in terms of classification accuracy. “Weighted average” and “Multi-head Attention” denotes different choices of the MPE module. The bold font and the underline indicate the best and the second-best results respectively. For simplicity and fewer parameters, we apply the weighted average as our default setting.

Method	HMDB51	UCF101	Kinetics
TRX [33]	9.3	16.9	16.8
STRM [43]	7.2	12.0	11.0
MORN	17.4	24.4	26.9

Table 2. Average PRIDE values across prototypes computed in C_{novel} on HMDB51, UCF101 and Kinetics. MORN achieves the best results on all three datasets.

4.1. Comparison with State-of-the-arts

As shown in Tab. 1, we comprehensively compare four datasets for the standard 5-way 5-shot action recognition task with state-of-the-art methods. Using a multi-head attention mechanism with 8 heads as the MPE module, our proposed MORN achieves the best results of 87.1% on HMDB51, 97.7% on UCF101 and 94.6% on Kinetics and the second-best result of 71.7% on SSv2. A more detailed ablation study of the MPE module will be illustrated in Sec. 4.3. CPMT [19] uses both object features and compound prototypes, thus achieves the best results before us on HMDB51, Kinetics and SSv2. It indicates the importance of multimodal information and representative prototypes. Compared to CPMT, we use the semantic information of label texts and an MPE module to achieve performance gains on HMDB51, UCF101 and Kinetics but a descent on SSv2. It is probably because some label texts in SSv2 are so similar that it is hard to discriminate them, *e.g. pouring something into something* against *pouring something onto something*. The more complex object features are more helpful in this case. In summary, MORN achieves the best results of 86.5% and 87.8% with the weighted average and the multi-head attention on average.

4.2. Multimodal Prototype-Enhanced Analysis

In this subsection, we explore the performance of our multimodal prototype-enhanced strategy. As mentioned earlier, we use PRIDE to evaluate the quality of prototypes, and further analysis shows the correlation between PRIDE and accuracy.

We randomly sample 10000 test episodes to compute PRIDE values. As shown in Tab. 2, MORN achieves the highest PRIDE values of 17.4%, 24.4% and 26.9% on HMDB51, UCF101 and Kinetics and significant gains over TRX. Besides, we also compute the PRIDE values of STRM. STRM proposes a patch-level and a frame-level enrichment module based on TRX. However, STRM utilizes enrichment modules on the feature level, and we find it performs worse than TRX on our PRIDE evaluation metric. It is mainly because STRM only focuses on obtaining more reliable features rather than computing more representative prototypes. The results correspond with our motivation for PRIDE and demonstrate the effectiveness of PRIDE. In addition, there exists a certain positive correlation between PRIDE and accuracy which will be discussed in detail below. The comparison demonstrates that focusing on representative prototypes is of great necessity.

To explore the correlation between PRIDE and accuracy, we conduct an experiment of performance gains and correlation analysis of PRIDE and accuracy on each category of HMDB51. We randomly sample 10000 test episodes to compute accuracy and PRIDE values. As shown in Fig. 3a and 3b, MORN achieves significant gains on both PRIDE and accuracy. Furthermore, we find the two evaluation metrics follow a similar pattern, *e.g. pushup* ranks top-2 on PRIDE and top-1 on accuracy. To further verify the correlation between the two metrics, we conduct a Pearson correlation analysis between PRIDE and accuracy as shown in Fig. 3c. We find that 44% of the variance can be explained by a positive linear correlation between PRIDE and

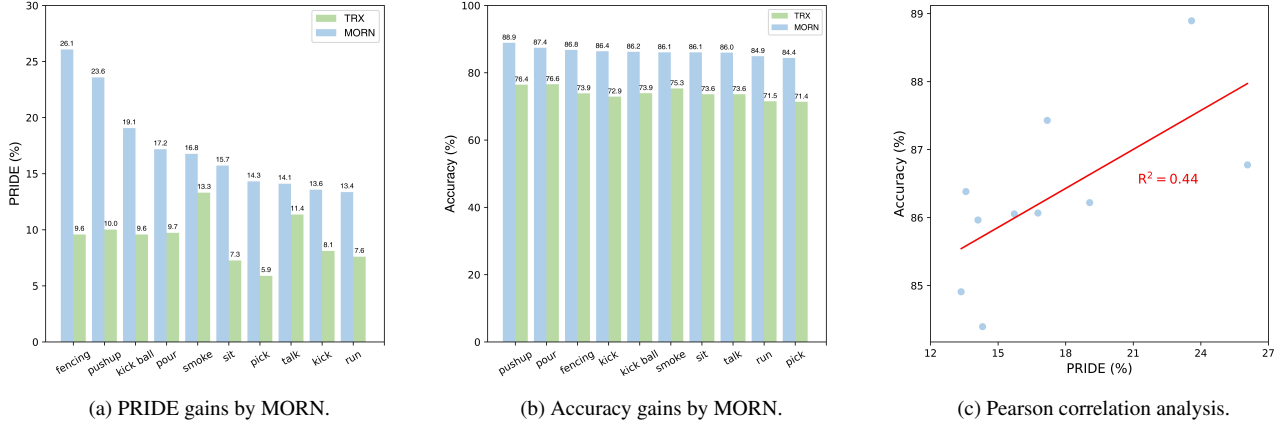


Figure 3. Performance gains and correlation analysis of PRIDE and accuracy on HMDB51. MORN achieves PRIDE gains in (a) and accuracy gains in (b) in each category. (c) is a Pearson correlation analysis between PRIDE and accuracy, showing a positive correlation.

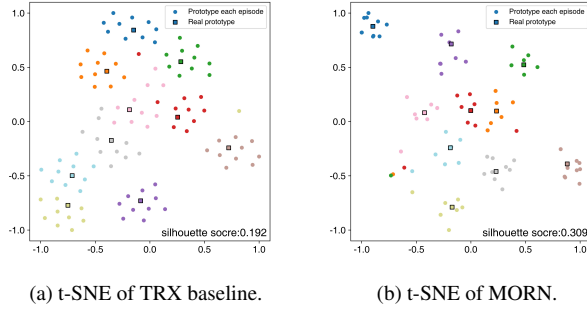


Figure 4. t-SNE [45] projection of prototypes of each episode and real prototypes on HMDB51. Our proposed MORN in (b) has a better category separability and a higher silhouette value than TRX baseline in (a).

accuracy. Our results further demonstrate the rationality of our proposed PRIDE evaluation metric and that PRIDE can complement the accuracy evaluation.

Intuitively, a method with a higher PRIDE value means a better discriminating performance against various categories. We randomly sample 10 prototypes in each category and the corresponding real prototypes. Then, we visualize the clusters by t-SNE [45] as shown in Fig. 4. Compared to TRX baseline, MORN has a better category separability, and prototypes are closer to the real prototypes. To quantify the results, we compute the silhouette values of the two methods. MORN outperforms TRX by 0.117, showing that MORN computes more representative prototypes for classification.

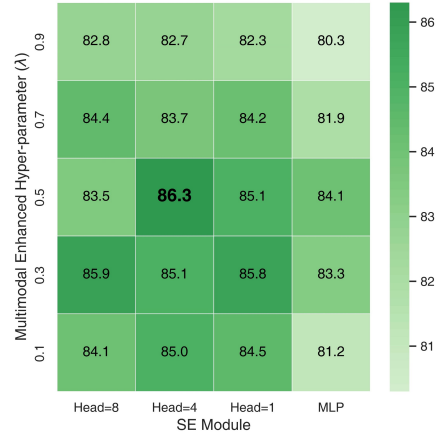


Figure 5. Ablation study of varying the SE module and the multimodal enhanced hyper-parameter (λ) on HMDB51. We utilize a multi-head attention mechanism with 4 heads as the SE module and set the multimodal enhanced hyper-parameter as 0.5.

4.3. Ablation Study

Design choices. As shown in Fig. 5, we compare various choices of the SE module and the multimodal enhanced hyper-parameter (λ) on HMDB51. When a two-layer MLP with a 1024-dimensional hidden layer is used as the SE module, we obtain the lowest and second-lowest classification accuracy with different multimodal enhanced hyper-parameter choices. It is mainly because the MLP has a relatively simple architecture and thus fails to fully explore the semantic information of label texts. Therefore, we focus on the multi-head attention mechanism [46]. As the head number increases, the fitting ability of the SE module improves

MPE module	HMDB51	UCF101	Kinetics
Concat + MLP	62.0	79.9	76.6
MLP + Concat	72.4	86.3	80.5
Weighted average	<u>86.3</u>	<u>96.9</u>	91.6
Head = 1	81	95.5	91.8
Head = 4	85.1	96.9	94.1
Head = 8	87.1	97.7	94.6

Table 3. Ablation study of the MPE module on HMDB51, UCF101 and Kinetics. ‘‘Concat’’ indicates a concatenation operation and ‘‘Head’’ indicates the head number in the multi-head attention mechanism. The bold font and the underline indicate the best and the second-best results respectively. With a multi-head attention mechanism, MORN can further improve its performance.

Method	HMDB51	UCF101	Kinetics
TRX [33]	75.6	96.1	85.9
MORN (w/o text flow)	77.9	95.9	86.7
MORN	86.3	96.9	91.6

Table 4. Ablation study of the multimodal information on HMDB51, UCF101 and Kinetics. MORN achieves significant gains with the semantic information of label texts.

as well. However, the classification accuracy fluctuates based on different head numbers and multimodal enhanced hyper-parameter choices. Firstly, the multimodal enhanced hyper-parameter determines the combination level of two modalities and is influenced by the specific scenario. Furthermore, the overfitting problem is more likely to arise in the few-shot scenario because of the scarcity of samples. We need to balance the trade-off between head numbers and multimodal enhanced hyper-parameter choices. According to our results, we utilize a multi-head attention mechanism with 4 heads as the SE module and set the multimodal enhanced hyper-parameter as 0.5 in our further experiments.

For the MPE module, applying a multi-head attention mechanism can further improve the performance of MORN as shown in Tab. 3. It turns out that the multimodal information can further enhance the prototypes with a better multimodal combination strategy. Although the weighted average is relatively simple with no parameters for training, our MORN with the weighted average can also achieve the second-best results of 86.3% on HMDB51 and 96.9% on UCF101, which has already outperformed those of prior methods. For simplicity and fewer parameters for training, we use the weighted average as our default MPE module.

Multimodal information. We employ the semantic information of label texts as an extra modality. To verify the importance of the multimodal information, we remove the text flow and replace the original ResNet-50 with a CLIP ResNet-50 in TRX. Different from the original ResNet-50, CLIP replaces the average pooling layer with an atten-

SE module (exist or not)	CLIP text encoder (freeze or not)	HMDB51	UCF101	Kinetics
✗	✗	84.5	96.1	88.8
✗	✓	83.9	96.4	90.6
✓	✗	76.7	93.2	87.2
✓	✓	86.3	96.9	91.6

Table 5. Ablation study of the SE module and the CLIP text encoder on HMDB51, UCF101 and Kinetics. With the SE module and a frozen CLIP text encoder, MORN achieves the best results on all three datasets.

tion pooling layer. We make no modifications to the CLIP ResNet-50 to avoid *catastrophic forgetting* [29], which refers to the performance decline of the pre-trained model. As shown in Tab. 4, the model achieves similar performance as TRX when removing the text flow. Specifically, the model achieves performance gains of 2.3% on HMDB51 and 0.8% on Kinetics, but a descent of 0.2% on UCF101 without the text flow. However, MORN achieves significant gains of 10.7%, 0.8% and 5.7% on HMDB51, UCF101 and Kinetics over those of TRX respectively, which verifies the importance of the semantic information of label texts.

SE module and CLIP text encoder. In the text flow, we first introduce a frozen CLIP text encoder. Then, a semantic-enhanced (SE) module is used to obtain text features with more reliable semantic information. As shown in Tab. 5, MORN with the SE module and a frozen CLIP text encoder achieves the best results on HMDB51, UCF101 and Kinetics. On the one hand, the function of the SE module is similar to that of the enrichment module in [43], which is used to enrich the semantic information. On the other hand, a frozen language encoder is proven to be effective in several works [36, 44] and our results further prove it. The above two modules function together and help MORN perform better. When we remove the SE module, the results are similar and are lower than MORN whether we freeze the CLIP text encoder or not. Besides, using the SE module and fine-tuning the CLIP text encoder leads to the lowest results on all three datasets. It is mainly because the overfitting problem becomes more serious as the parameters increase during training. Our results indicate the importance of the SE module and a frozen CLIP text encoder.

5. Conclusion

We propose a novel Multimodal Prototype-Enhanced Network (MORN) for few-shot action recognition. Besides, we are the first to propose a prototype evaluation metric called Prototype Similarity Difference (PRIDE) to the best of our knowledge. Our MORN uses the semantic information of label texts as multimodal information to compute more representative prototypes. Then, we use PRIDE

to evaluate multimodal prototypes and analyze the correlation between PRIDE and accuracy. MORN achieves state-of-the-art results, and our experiments show the importance of both the multimodal information and the prototype-enhanced network.

Limitations. Our MORN only applies TRX as baseline. In the future, we are interested in extending our MORN to more prototype-based methods and further applying our PRIDE evaluation metric.

References

- [1] Marcin Andrychowicz, Misha Denil, Sergio Gomez, Matthew W Hoffman, David Pfau, Tom Schaul, Brendan Shillingford, and Nando De Freitas. Learning to learn by gradient descent by gradient descent. *NeurIPS*, 29, 2016. 2
- [2] Antreas Antoniou, Harrison Edwards, and Amos Storkey. How to train your maml. *ICLR*, 2018. 2
- [3] Mina Bishay, Georgios Zoumpoulis, and Ioannis Patras. Tarn: Temporal attentive relation network for few-shot and zero-shot action recognition. *BMVC*, page 154, 2019. 1, 3
- [4] Kaidi Cao, Jingwei Ji, Zhangjie Cao, Chien-Yi Chang, and Juan Carlos Nieves. Few-shot video classification via temporal alignment. In *CVPR*, pages 10618–10627, 2020. 1, 3, 5, 6
- [5] Joao Carreira and Andrew Zisserman. Quo vadis, action recognition? a new model and the kinetics dataset. In *CVPR*, pages 6299–6308, 2017. 5
- [6] Zitian Chen, Yanwei Fu, Yinda Zhang, Yu-Gang Jiang, Xiangyang Xue, and Leonid Sigal. Semantic feature augmentation in few-shot learning. *arXiv preprint arXiv:1804.05298*, 86(89):2, 2018. 2
- [7] Zitian Chen, Yanwei Fu, Yinda Zhang, Yu-Gang Jiang, Xiangyang Xue, and Leonid Sigal. Multi-level semantic feature augmentation for one-shot learning. *IEEE Transactions on Image Processing*, 28(9):4594–4605, 2019. 2
- [8] Jia Deng, Wei Dong, Richard Socher, Li-Jia Li, Kai Li, and Li Fei-Fei. Imagenet: A large-scale hierarchical image database. In *CVPR*, pages 248–255, 2009. 5
- [9] Carl Doersch, Ankush Gupta, and Andrew Zisserman. Crosstransformers: spatially-aware few-shot transfer. *NeurIPS*, 33:21981–21993, 2020. 3, 4
- [10] Chelsea Finn, Pieter Abbeel, and Sergey Levine. Model-agnostic meta-learning for fast adaptation of deep networks. In *ICML*, pages 1126–1135, 2017. 2
- [11] Yuqian Fu, Li Zhang, Junke Wang, Yanwei Fu, and Yu-Gang Jiang. Depth guided adaptive meta-fusion network for few-shot video recognition. In *ACMMM*, pages 1142–1151, 2020. 1, 2, 3
- [12] Peng Gao, Shijie Geng, Renrui Zhang, Teli Ma, Rongyao Fang, Yongfeng Zhang, Hongsheng Li, and Yu Qiao. Clip-adapter: Better vision-language models with feature adapters. *arXiv preprint arXiv:2110.04544*, 2021. 2
- [13] Victor Garcia and Joan Bruna. Few-shot learning with graph neural networks. *ICLR*, 2018. 3
- [14] Ian Goodfellow, Jean Pouget-Abadie, Mehdi Mirza, Bing Xu, David Warde-Farley, Sherjil Ozair, Aaron Courville, and Yoshua Bengio. Generative adversarial networks. *Communications of the ACM*, 63(11):139–144, 2020. 2
- [15] Raghav Goyal, Samira Ebrahimi Kahou, Vincent Michalski, Joanna Materzynska, Susanne Westphal, Heuna Kim, Valentin Haenel, Ingo Fruend, Peter Yianilos, Moritz Mueller-Freitag, et al. The” something something” video database for learning and evaluating visual common sense. In *ICCV*, pages 5842–5850, 2017. 5
- [16] LiangYan Gui, YuXiong Wang, Deva Ramanan, and José MF Moura. Few-shot human motion prediction via meta-learning. In *ECCV*, pages 432–450, 2018. 2
- [17] Kaiming He, Xiangyu Zhang, Shaoqing Ren, and Jian Sun. Deep residual learning for image recognition. In *CVPR*, pages 770–778, 2016. 5
- [18] Ruibing Hou, Hong Chang, Bingpeng Ma, Shiguang Shan, and Xilin Chen. Cross attention network for few-shot classification. *NeurIPS*, 32, 2019. 3
- [19] Yifei Huang, Lijin Yang, and Yoichi Sato. Compound prototype matching for few-shot action recognition. *ECCV*, 2022. 1, 3, 5, 6
- [20] Muhammad Abdullah Jamal and Guo-Jun Qi. Task agnostic meta-learning for few-shot learning. In *CVPR*, pages 11719–11727, 2019. 2
- [21] Jongmin Kim, Taesup Kim, Sungwoong Kim, and Chang D Yoo. Edge-labeling graph neural network for few-shot learning. In *CVPR*, pages 11–20, 2019. 3
- [22] Hildegard Kuehne, Hueihan Jhuang, Estíbaliz Garrote, Tomaso Poggio, and Thomas Serre. Hmdb: a large video database for human motion recognition. In *ICCV*, pages 2556–2563, 2011. 5
- [23] Sai Kumar Dwivedi, Vikram Gupta, Rahul Mitra, Shuaib Ahmed, and Arjun Jain. Protogan: Towards few shot learning for action recognition. In *CVPRW*, 2019. 1, 2, 3
- [24] Kwonjoon Lee, Subhansu Maji, Avinash Ravichandran, and Stefano Soatto. Meta-learning with differentiable convex optimization. In *CVPR*, pages 10657–10665, 2019. 2
- [25] Hongyang Li, David Eigen, Samuel Dodge, Matthew Zeiler, and Xiaogang Wang. Finding task-relevant features for few-shot learning by category traversal. In *CVPR*, pages 1–10, 2019. 3
- [26] Rex Liu, Huanle Zhang, Hamed Pirsiavash, and Xin Liu. Mastaf: A spatio-temporal attention fusion network for few-shot video classification. *arXiv preprint arXiv:2112.04585*, 2021. 1, 3
- [27] Yaoyao Liu, Bernt Schiele, and Qianru Sun. An ensemble of epoch-wise empirical bayes for few-shot learning. In *ECCV*, pages 404–421, 2020. 2
- [28] Ilya Loshchilov and Frank Hutter. Decoupled weight decay regularization. *arXiv preprint arXiv:1711.05101*, 2017. 5
- [29] Michael McCloskey and Neal J Cohen. Catastrophic interference in connectionist networks: The sequential learning problem. In *Psychology of learning and motivation*, volume 24, pages 109–165. Elsevier, 1989. 8
- [30] Frederik Pahde, Oleksiy Ostapenko, Patrick Jä Hnichen, Tasilo Klein, and Moin Nabi. Self-paced adversarial training for multimodal few-shot learning. In *WACV*, pages 218–226, 2019. 2

- [31] Frederik Pahde, Mihai Puscas, Tassilo Klein, and Moin Nabi. Multimodal prototypical networks for few-shot learning. In *WACV*, pages 2644–2653, 2021. 2
- [32] Luis Perez and Jason Wang. The effectiveness of data augmentation in image classification using deep learning. *arXiv preprint arXiv:1712.04621*, 2017. 2
- [33] Toby Perrett, Alessandro Masullo, Tilo Burghardt, Majid Mirmehdi, and Dima Damen. Temporal-relational crosstransformers for few-shot action recognition. In *CVPR*, pages 475–484, 2021. 1, 2, 3, 4, 5, 6, 8
- [34] Alec Radford, Jong Wook Kim, Chris Hallacy, Aditya Ramesh, Gabriel Goh, Sandhini Agarwal, Girish Sastry, Amanda Askell, Pamela Mishkin, Jack Clark, et al. Learning transferable visual models from natural language supervision. In *ICML*, pages 8748–8763, 2021. 2
- [35] Alec Radford, Jeffrey Wu, Rewon Child, David Luan, Dario Amodei, Ilya Sutskever, et al. Language models are unsupervised multitask learners. *OpenAI blog*, 1(8):9, 2019. 5
- [36] Yongming Rao, Wenliang Zhao, Guangyi Chen, Yansong Tang, Zheng Zhu, Guan Huang, Jie Zhou, and Jiwen Lu. Denseclip: Language-guided dense prediction with context-aware prompting. In *CVPR*, pages 18082–18091, 2022. 5, 8
- [37] Alexander J Ratner, Henry Ehrenberg, Zeshan Hussain, Jared Dunnmon, and Christopher Ré. Learning to compose domain-specific transformations for data augmentation. *NeurIPS*, 30, 2017. 2
- [38] Sachin Ravi and Hugo Larochelle. Optimization as a model for few-shot learning. *ICLR*, 2017. 2
- [39] Jake Snell, Kevin Swersky, and Richard Zemel. Prototypical networks for few-shot learning. *NeurIPS*, 30, 2017. 1, 3
- [40] Khurram Soomro, Amir Roshan Zamir, and Mubarak Shah. Ucf101: A dataset of 101 human actions classes from videos in the wild. *arXiv preprint arXiv:1212.0402*, 2012. 5
- [41] Qianru Sun, Yaoyao Liu, Tat-Seng Chua, and Bernt Schiele. Meta-transfer learning for few-shot learning. In *CVPR*, pages 403–412, 2019. 2
- [42] Flood Sung, Yongxin Yang, Li Zhang, Tao Xiang, Philip HS Torr, and Timothy M Hospedales. Learning to compare: Relation network for few-shot learning. In *CVPR*, pages 1199–1208, 2018. 3
- [43] Anirudh Thatipelli, Sanath Narayan, Salman Khan, Rao Muhammad Anwer, Fahad Shahbaz Khan, and Bernard Ghanem. Spatio-temporal relation modeling for few-shot action recognition. In *CVPR*, pages 19958–19967, 2022. 1, 3, 5, 6, 8
- [44] Maria Tsimpoukelli, Jacob L Menick, Serkan Cabi, SM Eslami, Oriol Vinyals, and Felix Hill. Multimodal few-shot learning with frozen language models. *NeurIPS*, 34:200–212, 2021. 8
- [45] Laurens Van der Maaten and Geoffrey Hinton. Visualizing data using t-sne. *Journal of machine learning research*, 9(11), 2008. 7
- [46] Ashish Vaswani, Noam Shazeer, Niki Parmar, Jakob Uszkoreit, Llion Jones, Aidan N Gomez, Łukasz Kaiser, and Illia Polosukhin. Attention is all you need. *NeurIPS*, 30, 2017. 5, 7
- [47] Oriol Vinyals, Charles Blundell, Timothy Lillicrap, Daan Wierstra, et al. Matching networks for one shot learning. *NeurIPS*, 29, 2016. 3, 4
- [48] Limin Wang, Yuanjun Xiong, Zhe Wang, Yu Qiao, Dahua Lin, Xiaoou Tang, and Luc Van Gool. Temporal segment networks: Towards good practices for deep action recognition. In *ECCV*, pages 20–36, 2016. 4, 5
- [49] Mengmeng Wang, Jiazheng Xing, and Yong Liu. Actionclip: A new paradigm for video action recognition. *arXiv preprint arXiv:2109.08472*, 2021. 2
- [50] Xiang Wang, Shiwei Zhang, Zhiwu Qing, Mingqian Tang, Zhengrong Zuo, Changxin Gao, Rong Jin, and Nong Sang. Hybrid relation guided set matching for few-shot action recognition. In *CVPR*, pages 19948–19957, 2022. 1, 3, 5, 6
- [51] Jiamin Wu, Tianzhu Zhang, Zhe Zhang, Feng Wu, and Yongdong Zhang. Motion-modulated temporal fragment alignment network for few-shot action recognition. In *CVPR*, pages 9151–9160, 2022. 1, 3, 5, 6
- [52] Ling Yang, Liangliang Li, Zilun Zhang, Xinyu Zhou, Erjin Zhou, and Yu Liu. Dpgn: Distribution propagation graph network for few-shot learning. In *CVPR*, pages 13390–13399, 2020. 3
- [53] Han-Jia Ye, Hexiang Hu, De-Chuan Zhan, and Fei Sha. Few-shot learning via embedding adaptation with set-to-set functions. In *CVPR*, pages 8808–8817, 2020. 3
- [54] Sung Whan Yoon, Jun Seo, and Jaekyun Moon. Tapnet: Neural network augmented with task-adaptive projection for few-shot learning. In *ICML*, pages 7115–7123, 2019. 3
- [55] Baoquan Zhang, Xutao Li, Yunming Ye, Zhichao Huang, and Lisai Zhang. Prototype completion with primitive knowledge for few-shot learning. In *CVPR*, pages 3754–3762, 2021. 2, 5
- [56] Hongguang Zhang, Li Zhang, Xiaojuan Qi, Hongdong Li, Philip HS Torr, and Piotr Koniusz. Few-shot action recognition with permutation-invariant attention. In *ECCV*, pages 525–542, 2020. 1, 3, 5, 6
- [57] Lingling Zhang, Xiaojun Chang, Jun Liu, Minnan Luo, Mahesh Prakash, and Alexander G Hauptmann. Few-shot activity recognition with cross-modal memory network. *PR*, 108:107348, 2020. 1, 2, 3
- [58] Renrui Zhang, Rongyao Fang, Peng Gao, Wei Zhang, Kunchang Li, Jifeng Dai, Yu Qiao, and Hongsheng Li. Tip-adapter: Training-free clip-adapter for better vision-language modeling. *arXiv preprint arXiv:2111.03930*, 2021. 2
- [59] Songyang Zhang, Jiale Zhou, and Xuming He. Learning implicit temporal alignment for few-shot video classification. *IJCAI*, 2021. 1, 3
- [60] Kaiyang Zhou, Jingkang Yang, Chen Change Loy, and Ziwei Liu. Learning to prompt for vision-language models. *IJCV*, pages 1–12, 2022. 2
- [61] Linchao Zhu and Yi Yang. Compound memory networks for few-shot video classification. In *ECCV*, pages 751–766, 2018. 1, 3, 5
- [62] Xiatian Zhu, Antoine Toisoul, Juan-Manuel Perez-Rua, Li Zhang, Brais Martinez, and Tao Xiang. Few-shot ac-

tion recognition with prototype-centered attentive learning.
BMVC, 2021. [1](#), [2](#), [3](#), [5](#), [6](#)